Hindawi
Shock and Vibration
Volume 2022, Article ID 8028599, 9 pages
https://doi.org/10.1155/2022/8028599

Research Article

Acoustic Fault Diagnosis of Rotor Bearing System

Yuwei Liu,[1] **Yuqiang Cheng**,[1] **Zhenzhen Zhang**,[2] **and Jianjun Wu**[1]

[1]*College of Aerospace Science and Engineering, National University of Defense Technology, Changsha 410008, China*
[2]*Xi'an Aerospace Propulsion Institute, Xi'an 710100, China*

Correspondence should be addressed to Yuqiang Cheng; cheng_yuqiang@163.com

Received 13 November 2021; Revised 23 March 2022; Accepted 30 March 2022; Published 23 April 2022

Academic Editor: S bastien Besset

Early diagnosis of failures can prevent financial losses and industry downtime. In this article, the author proposes an early fault diagnosis technique for rotor-bearing faults. The proposed technique is based on the recognition of sound signals. The author measured and analyzed the three states of the rotor-bearing system: the rotor-bearing system under normal operating conditions, the rotor-bearing system with faulty bearings, and the rotor-bearing system with rotor friction. In this article, an original feature extraction method is described, namely, the 1/3 doubling method (a method of selecting the amplitude of the frequency ratio that is a multiple of 30% of the maximum amplitude). This method is used to form feature vectors. A classification of the obtained vectors was performed by the KNN (K-nearest neighbor classifier), the SVM (support vector machine), and the decision tree. The method is also compared with the Fourier synchrosqueezed transform. The experimental results show that the method can diagnose early faults of rotor-bearing systems simply and quickly and can be used to protect the safe operation of mechanical equipment.

1. Introduction

Rotating machinery is the most widely used type of mechanical equipment in aerospace equipment. Bearings, as one of the core components of rotating machinery, affect the operation of mechanical equipment. According to statistics, about 40% of faults in mechanical equipment are caused by bearing faults, so it is of great significance to diagnose bearing faults [1]. At the same time, the impact of the rotor will always affect the normal operation of the entire system, causing unnecessary energy loss and even safety accidents.

During the operation of the rotor-bearing system, the operating conditions can be characterized by certain physical and chemical parameters, including vibration amplitude, vibration frequency, energy, force, temperature, and friction. These parameters will change regularly when the rotor-bearing equipment is in normal operation and faulty operation. Appropriate data processing methods are used to analyze the original signal, process and extract its most essential information change law, and then judge whether the rotor-bearing system is malfunctioning [2]. He et al. used acoustic emission signals for fault classification. Although short-time Fourier transform replaced signal processing and feature extraction techniques to reduce the time delay of data preprocessing, the accuracy of the model was seriously affected by irregular noise. Chen Yang et al. used the time-domain index of the vibration signal as the extracted feature and then combined the random forest method to select the margin as the most accurate fault diagnosis feature [3]. Hoang et al. chose the current signal of the motor itself, combined with a deep convolutional neural network and information fusion technology, to classify faults [4]. Cui et al. proposed a new coupled multistable stochastic resonance method based on the traditional stochastic co-oscillation (SR) using two heterodyne multistable stochastic co-oscillation systems. This method simplifies the complexity of the conventional SR in its parameter determination and allows adaptive optimization and determination of the system parameters of the SR [5]. In the follow-up study, Wu et al. proposed a fault diagnosis method based on cascaded adaptive second-order tristable stochastic resonance (CASTSR) and EMD for the problems of poor quality and extraction effects of empirical modal decomposition (EMD) decomposition of weak signals with strong noisy weak signals [6]. On the other hand, Zhao et al. proposed a feature extraction method based on a data-driven approach

for the problem of predicting the remaining useful life (RUL) of key components of rolling bearings. According to the experimental results, the developed RUL prediction model was able to accurately predict the RUL of rolling bearings [7].

For the acoustic signal, due to its low signal-to-noise ratio, there are defects such as difficulty in extracting fault features. A variety of noise reduction methods have emerged to address the problem of the low signal-to-noise ratio of sound signals. Donoho [8] et al. proposed the wavelet threshold denoising algorithm that distinguishes the signal from noise by setting an appropriate threshold. However, when the wavelet coefficients at a certain detail in the original signal are close to the wavelet coefficients with more noise, the useful signal is easy to be regarded as noise is filtered out. Li et al. [9] for the problem of long signal transmission paths of rolling bodies and difficult signal feature extraction. The optimized variational mode decomposition with kurtosis mean (KMVMD) and maximum correlated kurtosis deconvolution based on power spectrum entropy and grid search (PGMCKD) are used to achieve the extraction of weak signal features of rolling bodies. Therefore, researchers have proposed other improvements to this problem [10–16]. On the other hand, researchers use multiple sound receiving devices to improve the signal-to-noise ratio of sound signals. For example, Wen [17] et al. used and compared four different microphone phase arrays, and calculated the error and spatial resolution of different types of phase arrays so that the acoustic signal has a higher signal-to-noise ratio. Liu [18] et al. constructed a high-order sound field sensor array using vector sensors to improve the performance of azimuth estimation.

Although the abovementioned scholars use different signal types, different signal processing methods, and different feature extraction methods to diagnose equipment faults, acoustic signals, as a noncontact state detection method, can overcome the limitations of equipment structure. This leads to the disadvantage of inconvenient installation of the sensor. This makes acoustic signal fault detection popular.

In practice, engineering researchers need to be able to quickly and accurately detect faults and achieve fault isolation. This requires a simple and effective fault identification method. We proposed a fault identification method using only the fast Fourier transform and simple machine learning and compared the proposed method with the Fourier simultaneous compression transform analysis method by comparing the proposed method with the Fourier simultaneous compression transform. The experimental results show that the proposed method is able to diagnose rotor-bearing faults accurately and effectively compared to the Fourier simultaneous compression transform method. It has the advantages of rapidity, stability, and applicability.

2. Fault Diagnosis Technology Based on Acoustic Signal

The proposed acoustic signal-based fault diagnosis technology signal processing method includes preprocessing, feature extraction, and classification [19]. First, the recorded acoustic signals are divided into lengths of the n-th power of 2, so that the computer can process these signals faster. In this paper, the length of the 15th power of 2 (32768) acoustic signals is selected as the analysis signal. Then, divide the sound data into 1-second data files. After normalization in the range of [−1, 1], the signal is processed by the Hanning window, the fast Fourier transform (FFT) method, and the 1/3 frequency multiplication method. The feature extraction method calculates the training feature vector and the test feature vector as shown in Figure 1. Finally, the feature vector is classified based on the K-nearest neighbor classifier, support vector machine (SVM), and decision tree (DT).

2.1. Method of Selection of Amplitudes of the 1/3 Octave Method. Based on the processing of the fast Fourier transform spectrum of the acoustic signal of the rotor-bearing system, a 1/3 frequency multiplication method is proposed to extract features from the acoustic signal and analyze the difference of the state spectrum of the rotor-bearing system [20]. It is presented in the form of a flowchart, as shown in Figure 2.

The specific steps of the 1/3 frequency multiplication methods are as follows:

(1) The acoustic signals of different states of the rotor-bearing system collected by the sensor are subjected to segmentation processing and then subjected to the fast Fourier transform to obtain the frequency spectrum. The frequency spectrum of a normal rotor-bearing acoustic signal is expressed as a vector normal = [normal1, normal2, . . ., normal16384], and the frequency spectrum of an inner ring faulty rotor-bearing is expressed as a vector inner = [inner1,-inner2, . . ., inner16384], with an outer ring. The frequency spectrum of the failed rotor-bearing is expressed as outer = [outer1, outer2, . . ., outer16384], and the frequency spectrum of the rotor bearing with the rolling element failure is expressed as rolling = [rolling1, rolling2, . . ., -rolling16384], as well as those with rubbing faults. The rotor-bearing spectrum is expressed as rubbing = [rubbing1, rubbing2, . . ., rubbing16384].

(2) Calculate the frequency spectrum difference between the fault state and the normal state of the rotor rolling system: normal−inner, normal−outer, normal−rolling, normal-rubbing, inner−outer, inner−-rolling, inner-rubbing, outer−rolling, outer -rubbing, rolling-rubbing.

(3) Calculate the absolute value of the frequency spectrum difference between the fault state and the normal state of the rotor-bearing system: |normal−inner|, |normal−outer|, |normal−rolling|, |normal-rubbing|, |inner−outer|, |inner−rolling|, |inner-rubbing|, |outer −rolling|, |outer -rubbing|, |rolling-rubbing|.

(4) Find the frequency at which the absolute value of the frequency spectrum difference between each fault state and the normal state of the rotor-bearing

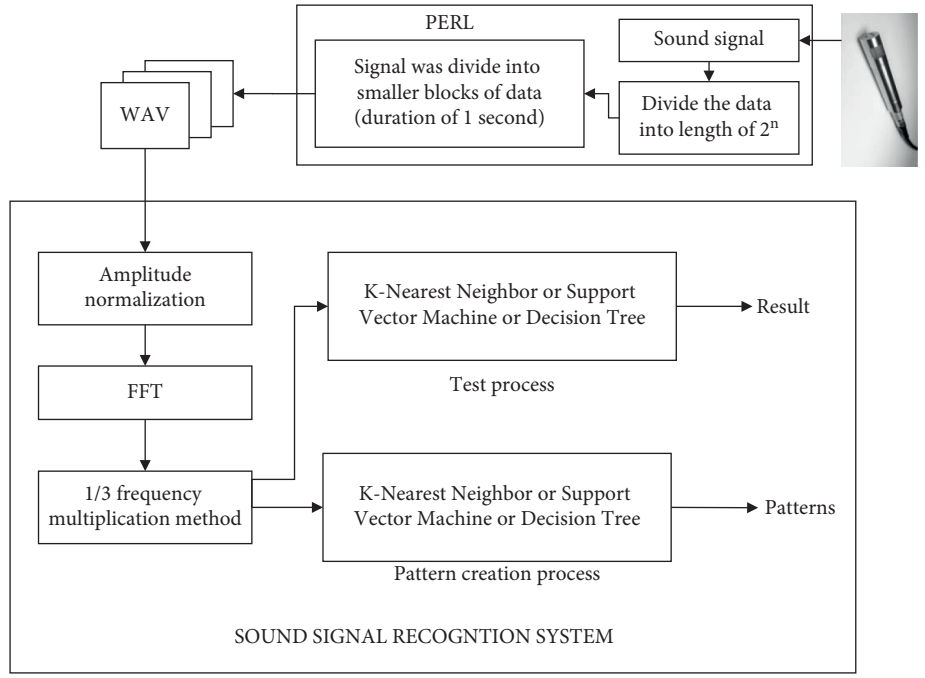

Figure 1: 1/3 octave method, K-nearest neighbor classifier, support vector machine, and decision tree based on the acoustic signal fault diagnosis technology flow chart.

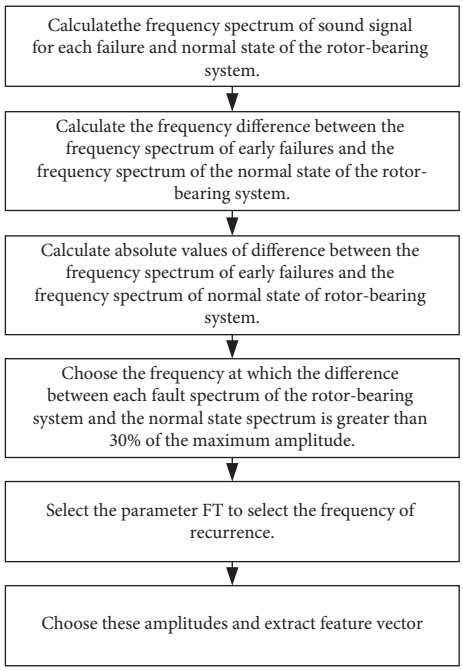

Figure 2: Flow chart of 1/3 frequency multiplication method.

system is greater than 30% of the maximum amplitude.

(5) Select the frequency number threshold FT. FT is defined as: FT = (the number of common frequency amplitudes selected)/(the number of frequency amplitudes in all states). For example, there is a training set, and each training set has five different states from A to E. We calculated 10 spectral differences. And the parameter FT is equal to 0.48, and $0.48 < 5/10 = 0.5$, the frequency that has repeated 5 times in the 10 spectrums is needed to determine the choice of the common frequency.

(6) Select these amplitudes to create the feature vector, using the rotor-bearing 1/3 frequency multiplication method, as shown in Figure 2.

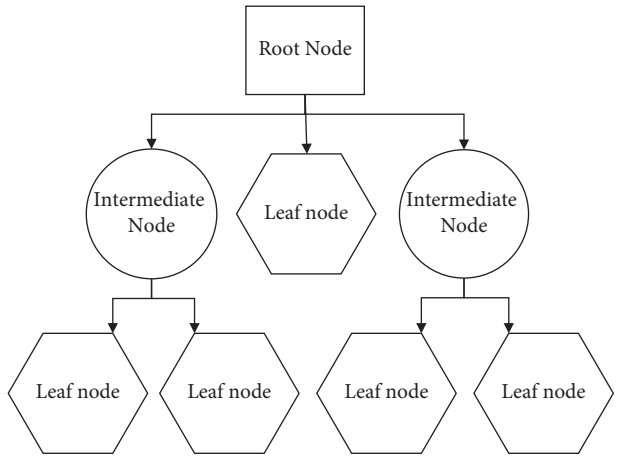

Figure 3: A diagram of the DT.

2.2. K-Nearest Neighbor Classifier. K-nearest neighbors, fuzzy logic, and neural network classification methods are all commonly used classification methods. The details of the K-nearest neighboring classifier are described in the

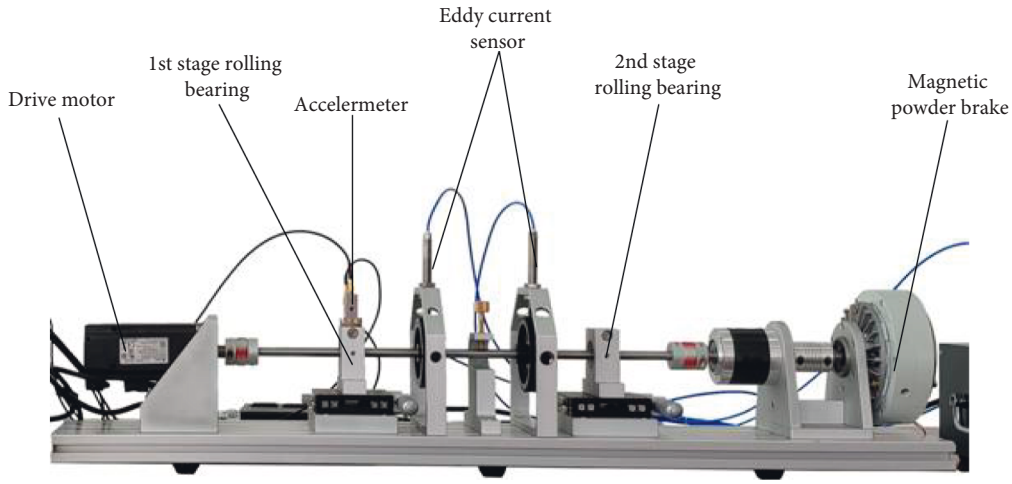

Figure 4: Experimental bench diagram.

literature [21–23], which is very suitable for classifying high-dimensional feature vectors. Euclidean distance is applied for the recognition of vibration signals of rolling element bearings, which is defined as the measurement of the distance between two feature vectors. For example, $P = [p_1, p_2, \ldots, p_n]$ and $C = [c_1, c_2, \ldots, c_n]$ are feature vectors with the same length of n. Then, d_e is the Euclidean distance that can be expressed as follows:

$$d_e(P, C) = \sqrt{\sum_{i=1}^{n} (p_i - c_i)^2}. \quad (1)$$

The test sample is determined through the majority decision rule, and the test sample is compared with the training samples. Then, the largest K neighbor number class is selected as the most recognizable class.

2.3. Support Vector Machine. A support vector machine (SVM), as a popular classification method, classifies feature vectors by finding the optimal solution of the formed hyperplane to separate the two types of vectors as much as possible [24]. And the hyperplane has the maximum distance between classified training vectors. The decision function can be presented as follows:

$$svm = \sum_{i} w_i f(sv_i, x) + q, \quad (2)$$

where w_i is the weights, f is the kernel function, sv_i is the support vectors, x is the feature vector, and q is the bias.

SVM has advantages such as being supported with vectors in the decision function and using different kernel functions for the decision function according to different conditions. More details about SVM can be found in the literature [25].

2.4. Decision Tree. Decision tree (DT) for a given dataset, the goal is to construct a model to capture the mechanism that produced the data. The structure of a decision tree consists of nodes, which are the points of the decision tree where attributes are tested, and branches, which are the test results leading to another node. The nodes are divided into a root node at the top, an internal node in the middle, and a leaf node at the end. A node is terminated if it meets the requirements of some predefined type (i.e., there is only one class output in that link). The basic task of building a decision tree is to repeatedly find the attributes to be tested at one node and then branch to another node. A diagram of the DT is shown in Figure 3. For more details on decision trees, please refer to the literature [26–28].

3. Experimental Data Analysis

To verify the effectiveness of the method, we conduct related experiments on the laboratory bench. The experimental platform is shown in Figure 4. In the experiment, the input speed of the rotor shaft was set at 1200 rpm, and the sampling frequency of the acoustic signal was set at 48000 Hz.

Differences between the failure frequency spectrum and the normal state of the rotor-bearing system at 1200 rpm are shown in Figures 5–14. In the analysis of this paper, 200 datasets were analyzed and was obtained through the data in addition, of which 20% were used for the test set.

4. Analysis of the Recognition Results of Acoustic Signals

This study selects five states of the acoustic signal of the rotor-bearing system, including normal state, inner ring failure state, outer ring failure state, rolling element failure state, and impact wear state. The rotor input speed is 1200 rpm, and the sampling rate is 48 kHz. The recognition efficiency of the acoustic signal can be calculated by the following formula:

$$E_F = \frac{N_p}{N_a} 100\%. \quad (3)$$

Among them, E_F is the recognition efficiency of acoustic signals, N_p is the number of test samples properly recognized, and N_a is the number of all test samples.

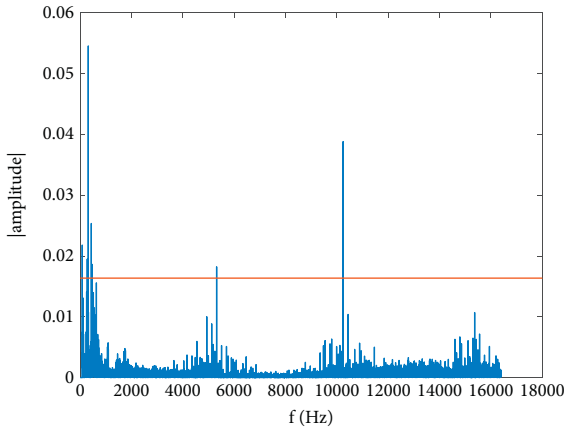

Figure 5: The spectra of frequencies of acoustic signal of |normal-inner|.

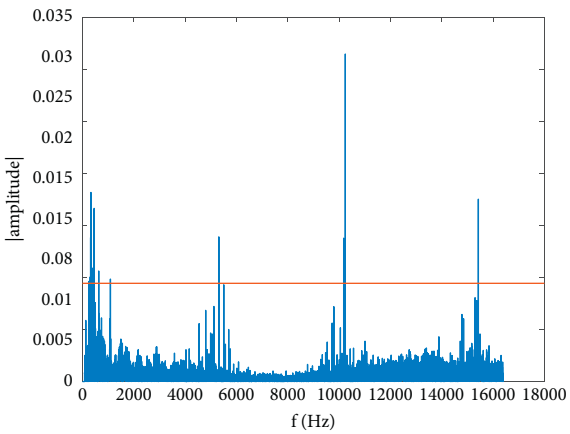

Figure 6: The spectra of frequencies of acoustic signal of |normal-outer|.

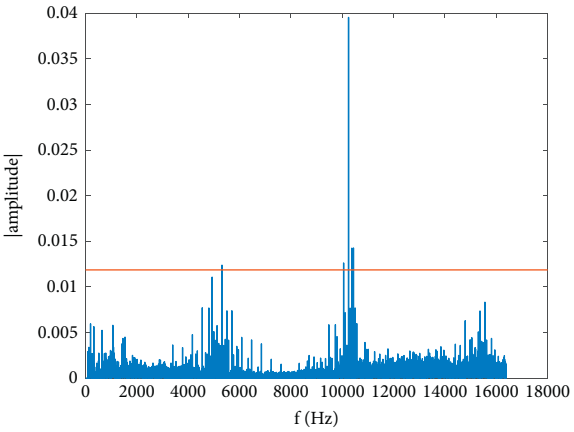

Figure 7: The spectra of frequencies of acoustic signal of |normal-rolling|.

The 1/3 octave method and the K-nearest neighbor recognition result of the acoustic signal are shown in Table 1, and the E_F value ranges from 93.5% to 100%.

The recognition results of the 1/3 frequency multiplication method and SVM on the acoustic signal are shown in Table 2, and the *EF* value is 85%~95%.

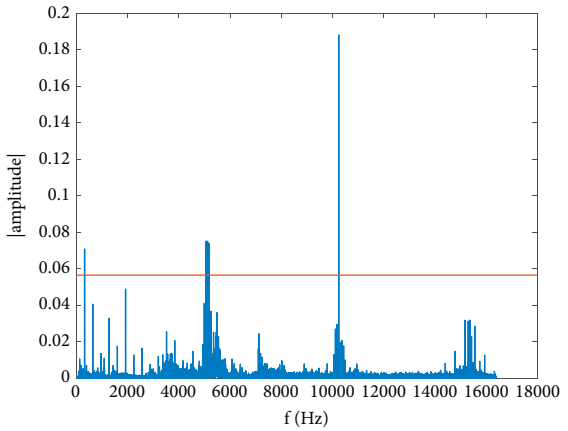

Figure 8: The spectra of frequencies of acoustic signal of |normal-rubbing|.

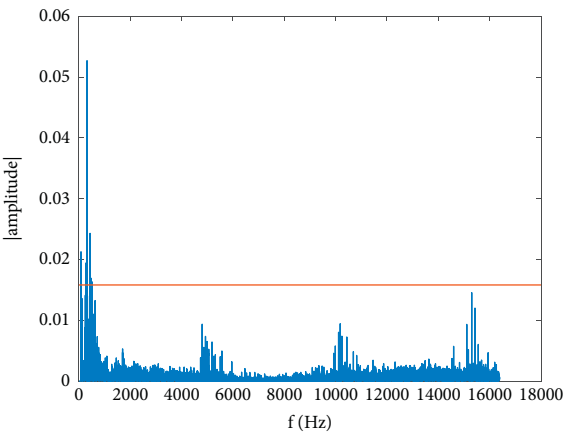

Figure 9: The spectra of frequencies of acoustic signal of |inner-outer|.

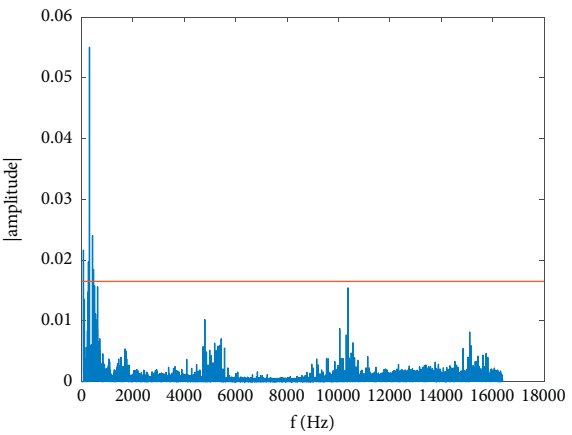

Figure 10: The spectra of frequencies of acoustic signal of |inner-rolling|.

The recognition results of the 1/3 octave method and the decision tree on the acoustic signal are shown in Table 3, and the EF value is 95%~100%.

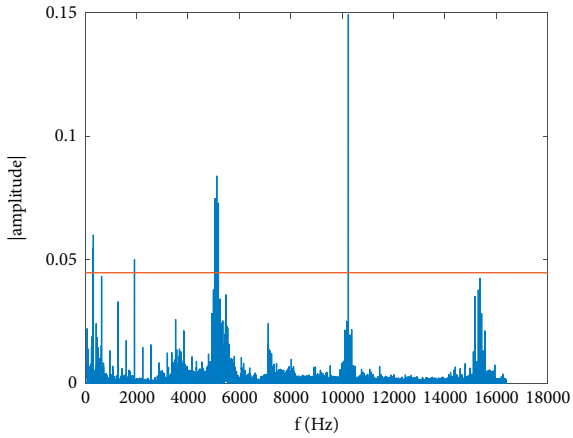

Figure 11: The spectra of frequencies of acoustic signal of |inner-rubbing|.

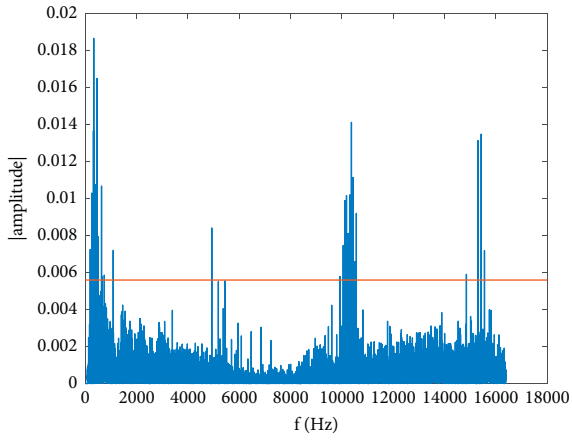

Figure 12: The spectra of frequencies of acoustic signal of |outer-rolling|.

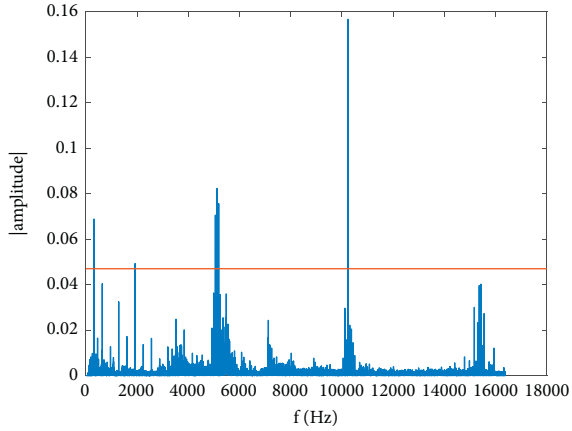

Figure 13: The spectra of frequencies of acoustic signal of |outer-rubbing|.

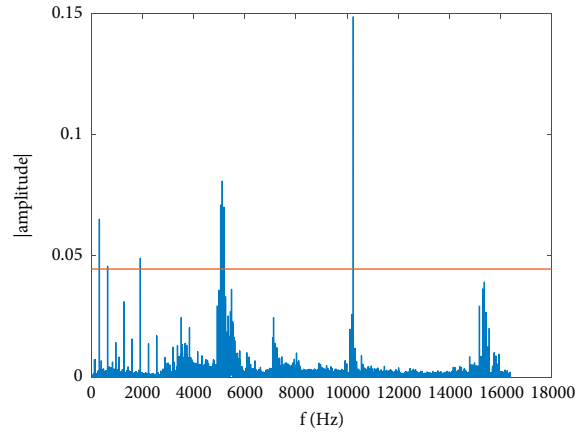

Figure 14: The spectra of frequencies of acoustic signal of |rolling-rubbing|.

Table 1: Recognition result of acoustic signals of rotor-bearing system with the 1/3 frequency multiplication method and the K-nearest neighboring classifier.

Type of acoustic signals	E_F (%)		
Number of K	1	3	5
Normal	100	100	100
Faulty inner ring	90	100	93.5
Faulty outer ring	100	100	100
Faulty rolling element	90	100	93.5
Rubbing	97	100	98.5

Table 2: Recognition results of acoustic signals of rotor-bearing system with the 1/3 frequency multiplication method and SVM.

Type of acoustic signals	E_F (%)
Normal	90
Faulty inner ring	95
Faulty outer ring	85
Faulty rolling element	85
Rubbing	93

Table 3: Recognition results of acoustic signals of rotor-bearing system with the 1/3 frequency multiplication method and decision tree.

Type of acoustic signals	E_F (%)
Normal	100
Faulty inner ring	95
Faulty outer ring	98
Faulty rolling element	98
Rubbing	100

5. Acoustic Fault Detection Method Based on the Time-Frequency Domain

To compare the effectiveness of the proposed method, the Fourier synchrosqueezed transform in the time-frequency domain is used in this subsection to analyze the acoustic signals. And the Fourier synchrosqueezed transform is

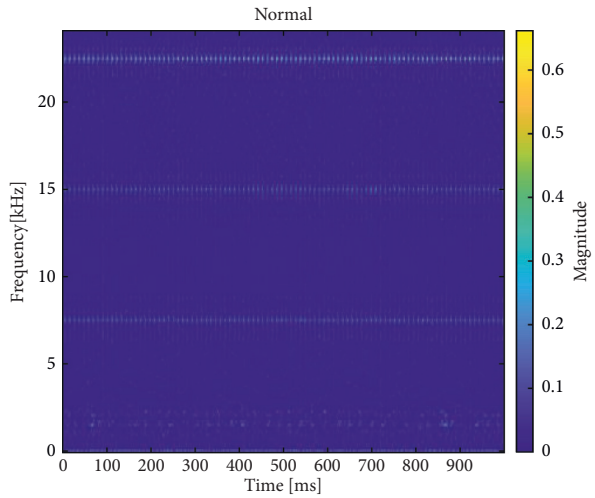

Figure 15: Fourier synchrosqueezed transform spectrum of normal signal.

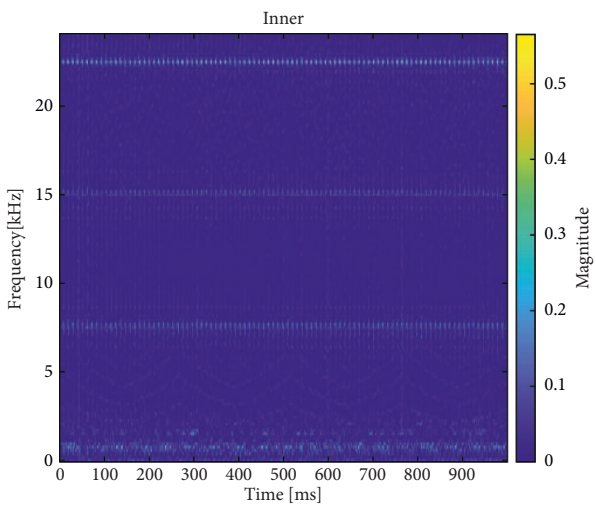

Figure 16: Fourier synchrosqueezed transform spectrum of inner ring fault signal.

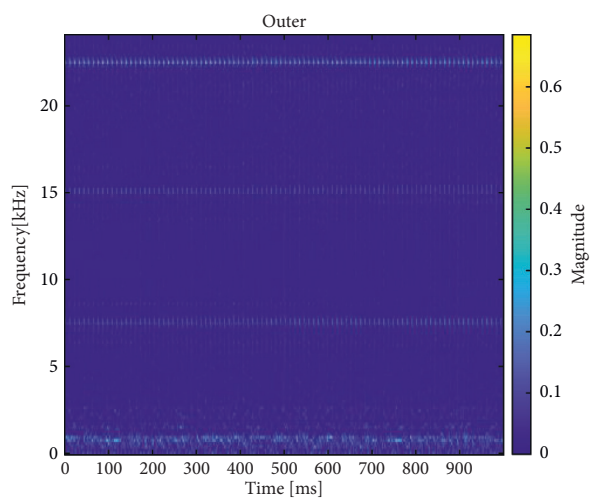

Figure 17: Fourier synchrosqueezed transform spectrum of outer ring fault signal.

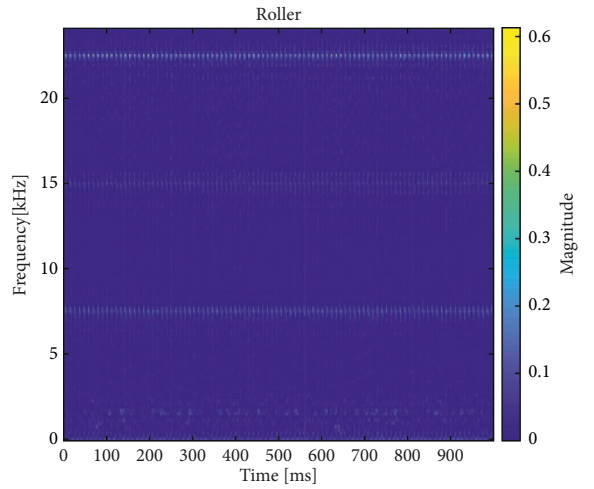

Figure 18: Fourier synchrosqueezed transform spectrum of roller fault signal.

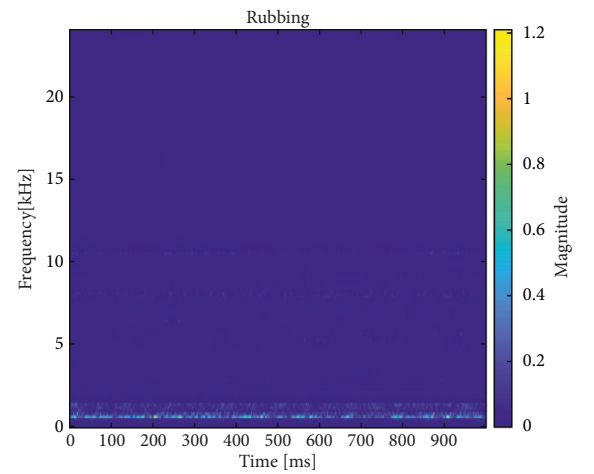

Figure 19: Fourier synchrosqueezed transform spectrum of rubbing signal.

performed on the acoustic signals of the abovementioned five states, respectively, and the results obtained are shown in Figures 15–19.

According to the analysis of Figures 15–19, first of all, from the five states, it can directly distinguish the rotor rubbing fault from other faults. In the other four states, signal after the Fourier synchronous transformation of the time-frequency results in the analysis of the four states of the high-frequency part of all three major peaks, but only from the Fourier synchronous pressure transformation of the acoustic signal obtained after the time-frequency spectrum, not effectively analyze the rolling bearing failure.

On the other hand, to test the effectiveness of the proposed method more comprehensively. We input the mean, standard deviation, cliffs, skewness, and peak-to-peak values from the time-domain statistical features of the collected signals as features into KNN, SVM, and DT for classification, and the obtained results are shown in Tables 4–6.

Table 4: Recognition result of acoustic signals of rotor-bearing system with time domain statistical characteristics and K-nearest neighboring classifier.

Type of acoustic signals	E_F (%)		
Number of K	1	3	5
Normal	90	90	90
Faulty inner ring	70	70	69
Faulty outer ring	50	51	52
Faulty rolling element	78	77	75
Rubbing	98	96	95

Table 5: Recognition results of acoustic signals of rotor-bearing system with time domain statistical characteristics and SVM.

Type of acoustic signals	E_F (%)
Normal	92
Faulty inner ring	76
Faulty outer ring	61
Faulty rolling element	85
Rubbing	97

Table 6: Recognition results of acoustic signals of rotor-bearing system with Time domain statistical characteristics and Decision Tree.

Type of acoustic signals	E_F (%)
Normal	92
Faulty inner ring	56
Faulty outer ring	60
Faulty rolling element	87
Rubbing	98

The results of time-domain statistical features and K-nearest neighbor identification of acoustic signals are shown in Table 4, with E_F averages of 76.86%.

The results of time-domain statistical features and K-nearest neighbor identification of acoustic signals are shown in Table 5, with E_F averages of 82.2%.

The results of time-domain statistical features and K-nearest neighbor identification of acoustic signals are shown in Table 6, with E_F averages of 78.4%.

From the results of the statistical features in the time-domain, the accuracy of the classification is not as high as that of the proposed method in this paper.

6. Conclusion

According to the results of fault identification, the feature extraction method of the 1/3 frequency multiplication method studied in this paper can effectively detect early rotor-bearing faults on the one hand and improve the identification efficiency of bearing vibration signals on the other hand. For the features extracted in this research, the decision number classifier is better than KNN and SVM. In contrast to other complex methods for extracting fault features through neural networks, the 1/3 frequency multiplication method requires only a fast Fourier transform to extract feature vectors that can effectively distinguish between different states and perform fault diagnosis. It can be used in engineering to monitor the condition of rotor bearings. However, the selection of the number of feature vectors, i.e., the size of FT, needs to be adjusted for different experimental situations and can be optimized and studied in the future.

Data Availability

The data used to support the findings of this study are included within the article.

Conflicts of Interest

The authors declare that there are no conflicts of interest regarding the publication of this paper.

References

[1] D. Y. Wu, Y. S. Wang, and Y. Li, "Overview of automobile engine fault diagnosis methods based on acoustic signals," *Journal of Bohai University (Natural Science Edition): Natural Science Edition*, vol. 29, no. 003, pp. 264–267, 2008, Chinese.

[2] M. He and D. He, "Deep learning based approach for bearing fault diagnosis," *IEEE Transactions on Industry Applications*, vol. 53, no. 3, pp. 3057–3065, 2017.

[3] C. Yang, L. Yi, Z. Shenguang, and L. Bo, "Fault diagnosis method of marine rolling bearing based on vibration time domain characteristics," *Machine tools and hydraulics*, vol. 49, no. 14, pp. 193–200, 2021, Chinese.

[4] D. T. Hoang and H. J. Kang, "A motor current signal-based bearing fault diagnosis using deep learning and information fusion," *IEEE Transactions on Instrumentation and Measurement*, vol. 69, no. 6, pp. 3325–3333, 2020.

[5] X. Ran, X. Zhou, M. Lei, W. Tepsan, and W. Deng, "A novel K-means clustering algorithm with a noise algorithm for capturing urban hotspots," *Applied Sciences*, vol. 11, no. 23, Article ID 11202, 2021.

[6] D. Wu, "fault diagnosis using cascaded adaptive second-order tristable stochastic resonance and empirical mode decomposition," *Applied Sciences*, vol. 11, 2021.

[7] H. Zhao, H. Liu, Y. Jin, X. Dang, and W. Deng, "Feature extraction for data-driven remaining useful life prediction of rolling bearings," *IEEE Transactions on Instrumentation and Measurement*, vol. 70, no. 99, pp. 1–10, 2021.

[8] S. D. Na, Q. Wei, Q. Wei, K. W. Seong, J. H. Cho, and M. N. Kim, "Noise reduction algorithm with the soft thresholding based on the Shannon entropy and bone-conduction speech cross- correlation bands," *Technology and Health Care: Official Journal of the European Society for Engineering and Medicine*, vol. 26, pp. 281–289, 2018.

[9] W. Li, Y. Li, L. Yu et al., "A novel fault feature extraction method for bearing rolling elements using optimized signal processing method," *Applied Sciences*, vol. 11, no. 19, 9095 pages, 2021.

[10] L. Dong-Han, A. Jong-Hyo, and K. Bong Hwan, "fault detection of bearing systems through EEMD and optimization algorithm," *Sensors*, vol. 172477 pages, 2017.

[11] L. Chen, G. Chen, and Z. Zhu, "Harmonic analysis method based on CEEMD-HT algorithm," *Electric Power Science and Engineering*, vol. 33, no. 1, pp. 61–66, 2017.

[12] M. E. Torres, M. A. Colominas, G. Schlotthauer, and P. A. Flandrin, "A complete ensemble empirical mode

decomposition with adaptive noise," in *Proceedings of the IEEE International Conference on Acoustics, Speech, and Signal Processing, ICASSP 2011*, pp. 4144–4147, IEEE, Prage, Czech Republic, May 2011.

[13] J. G. Wang, S. Chen, and C. Zhang, "Application and research of VMD and MCKD in bearing fault diagnosis," *Modular Machine Tool & Automatic Manufacturing Technique*, vol. 5, pp. 145–161, 2017.

[14] H. Zhao and L. I. Lang, "Incipient bearing fault diagnosis based on MCKD-EMD for wind turbine Electric Power," *Automation Equipment*, vol. 37, no. 2, pp. 29–36, 2017.

[15] Q. Wei, H. B. Wang, J. Yang, B. Feng, and A. M. Base, "Combination analysis on multi-characteristic parameters of aircraft generator fault diagnosis," *Measurement & Control Technology*, vol. 36, no. 7, pp. 47–51, 2017.

[16] Y. Liu, Y. Cheng, Z. Zhang, and J. Wu, "Multi-information fusion fault diagnosis based on KNN and improved evidence theory," *Journal of Vibration Engineering & Technologies*, vol. 11, pp. 1–12, 2021.

[17] W. Q. Jing, D. F. Comesaa, and P. C. David, "Sound source localization using a single acoustic vector sensor and multi-channel microphone phased arrays," in *Proceedings of the 43rd International Congress on Noise Control Engineering Internoise 2014*, Melbourne, Australia, November 2014.

[18] Y. Liu, Y. Wang, and Y. Yang, "Study of a super-resolution DOA estimation method for high-order acoustic sensor array," *Journal of Harbin Engineering University*, vol. 10, pp. 1–5, 2021.

[19] A. Glowacz, "Acoustic based fault diagnosis of three-phase induction motor," *Applied Acoustics*, vol. 137, pp. 82–89, 2018.

[20] A. Glowacz, W. Glowacz, Z. Glowacz, and J. Kozik, "Early fault diagnosis of bearing and stator faults of the single-phase induction motor using acoustic signals," *Measurement*, vol. 113, pp. 1–9, 2018.

[21] J. Vitola, F. Pozo, D. A. Tibaduiza, and M. Anaya, "A sensor data fusion system based on k-nearest neighbor pattern classification for structural health monitoring applications," *Sensors*, vol. 17, no. 2, 2017.

[22] J. Tian, C. Morillo, M. H. Azarian, and M. Pecht, "Motor bearing fault detection using spectral kurtosis-based feature extraction coupled with K-nearest neighbor distance analysis," *IEEE Transactions on Industrial Electronics*, vol. 63, no. 3, pp. 1793–1803, 2016.

[23] P. Baraldi, F. Cannarile, F. Di Maio, and E. Zio, "Hierarchical k-nearest neighbours classification and binary differential evolution for fault diagnostics of automotive bearings operating under variable conditions," *Engineering Applications of Artificial Intelligence*, vol. 56, pp. 1–13, 2016.

[24] A. Glowacz, "Fault diagnostics of DC motor using acoustic signals and MSAF-RATIO30-EXPANDED," *Archives of Electrical Engineering*, vol. 65, no. 4, pp. 733–744, 2016.

[25] D. H. Hwang, Y. W. Youn, J. H. Sun, K. H. Choi, J. H. Lee, and Y. H. Kim, "Support vector machine based bearing fault diagnosis for induction motors using vibration signals," *Journal of Electrical Engineering & Technology*, vol. 4, no. 10, pp. 1558–1565, 2015.

[26] S. Singh and P. Gupta, "Comparative study id3, cart and c4. 5 decision tree algorithm: a survey," *Int J Adv Inform Sci Technol (IJAIST)*, vol. 27, no. 27, pp. 97–103, 2014.

[27] K. Saleh and A. Ayad, "Fault zone identification and phase selection for microgrids using decision trees ensemble," *International Journal of Electrical Power & Energy Systems*, vol. 132, no. 132, Article ID 107178, 2021.

[28] M. Barrios Castellanos, A. L. Serpa, J. L. Biazussi, W. Monte Verde, and N. do Socorro Dias Arrifano Sassim, "Fault identification using a chain of decision trees in an electrical submersible pump operating in a liquid-gas flow," *Journal of Petroleum Science and Engineering*, vol. 184, Article ID 106490, 2020.